Research Square

Preprints are preliminary reports that have not undergone peer review.
They should not be considered conclusive, used to inform clinical practice,
or referenced by the media as validated information.

Anaplastic Transformation of Thyroid Follicular Adenoma Driven by TP53 and TERT Promoter Mutations with Triple-Tissue Sequencing Evidence

Huixuan Wang
The 960th Hospital of the PLA Joint Logistic Support Force
Yongcheng Cao
The 960th Hospital of the PLA Joint Logistic Support Force
Peifeng Li
lipeifeng00@hotmail.com
The 960th Hospital of the PLA Joint Logistic Support Force

Case Report

Keywords: Anaplastic thyroid carcinoma, Follicular adenoma, squamous cell carcinoma, TP53, TERT, HRAS

Posted Date: November 1st, 2026

DOI: https://doi.org/10.21203/rs.3.rs-10980420/v1

License: This work is licensed under a Creative Commons Attribution 4.0 International License. Read Full License

Additional Declarations: No competing interests reported.

Abstract

Anaplastic thyroid carcinoma (ATC) is a highly lethal malignancy that usually arises from pre-existing differentiated thyroid cancers, but direct transformation from a benign follicular adenoma has rarely been documented at the molecular level. We report an 83-year-old woman who experienced rapid enlargement of a long-standing thyroid nodule. Whole-exome and targeted sequencing provide direct in vivo evidence of clonal evolution from a follicular adenoma to ATC. The coexistence of follicular thyroid adenoma and ATC within the same nodule is exceedingly rare and, to our knowledge, has not been previously documented at the molecular level. Histological examination of the resection specimen revealed two distinct but adjacent components within the same nodule: follicular adenoma and anaplastic carcinoma (squamous cell carcinoma). Immunohistochemistry demonstrated gradual dedifferentiation from adenoma to anaplastic carcinoma, characterized by the absence of expression of thyroglobulin, thyroid transcription factor-1 and PAX-8, loss of E-cadherin expression, a mutant-pattern p53 staining, and an increase in the Ki-67 labeling index from 5% in the adenoma to > 60% in the anaplastic carcinoma. The squamous component was diffusely positive for p40 and CK5/6. Whole exome sequencing and thyroid-specific 12-gene panel testing revealed that in addition to a shared *HRAS* mutation, the anaplastic carcinoma uniquely harbored a *TP53* inactivating mutation and a *TERT* promoter activation mutation. These histological, immunohistochemical, and molecular genetic findings provide direct evidence that this case represents a direct transformation from follicular adenoma to anaplastic carcinoma.

Introduction

Anaplastic thyroid carcinoma accounts for only 1–2% of thyroid malignancies [1] but contributes disproportionately to thyroid cancer mortality, with a median survival of less than six months[2]. The prevailing model holds that most ATCs arise from pre-existing well-differentiated thyroid carcinomas through the stepwise accumulation of additional genetic alterations[3, 4], most notably *TP53* mutations and *TERT* promoter mutations [5]. Direct progression from a benign follicular adenoma to ATC, bypassing a clinically or histologically recognizable differentiated carcinoma stage, is exceptionally rare, and the molecular events underlying this shortcut have rarely been captured in a single patient.

We conducted whole-exome sequencing on samples of normal thyroid, follicular adenoma and anaplastic carcinoma from this patient. We also performed thyroid-specific 12-gene panel testing on the two tumor components. Combined with immunohistochemical analysis, we identified the critical genetic events associated with anaplastic transformation.

Case Presentation

An 83-year-old female presented with a thyroid nodule that had remained stable for many years but had undergone rapid enlargement over the preceding one month, and there was no family history of thyroid cancer. Physical examination revealed a firm, fixed mass in the right thyroid lobe. Ultrasound showed a mixed echoic nodule measuring 5.5 cm × 4.0 cm, with ill-defined borders. The patient subsequently underwent total thyroidectomy with bilateral modified radical neck dissection. The institutional ethics committee approved this study, and written informed consent was obtained from the patient.

Gross examination of the resection specimen disclosed a 5.5 cm × 4.0 cm ×4.0 cm mass. Serial sectioning revealed a well-circumscribed, encapsulated nodule with a thick fibrous capsule (0.2–0.3 cm in thickness). The majority of this nodule displayed a tan, homogeneous cut surface, consistent with a follicular adenoma. Within this adenoma, a discrete, ill-defined area was identified. This area was predominantly necrotic, with small amounts of gray-white, firm viable tumor tissue—gross features characteristic of anaplastic carcinoma arising within a pre-existing benign follicular neoplasm. (Fig. 1).

Histologically, two distinct components were identified (Fig. 2A-B): (1) a follicular adenoma surrounded by an intact fibrous capsule, composed of small-to-medium-sized follicles without capsular or vascular invasion; and (2) an anaplastic carcinoma composed of highly pleomorphic cells with squamous-cell features, brisk mitotic activity, and geographic necrosis. No distinct transitional zone was observed. Lymph node metastases were present in one of 40 examined nodes.

The two components exhibited distinct immunohistochemical profiles (Fig. 2C–J). Thyroid-lineage markers, including thyroglobulin, TTF-1, and PAX-8, were diffusely positive in the adenoma but markedly reduced or absent in the carcinoma. CK5/6 and p40 were negative in the adenoma but diffusely positive in the carcinoma.. p53 immunohistochemistry revealed a wild-type pattern—scattered, weak nuclear staining—in the adenoma tissues, and a mutant-type pattern—diffuse, strong nuclear positivity—in the anaplastic carcinoma. E-cadherin displayed crisp membranous staining in the adenoma but was largely lost in the anaplastic carcinoma. The Ki-67 labeling index increased from 5% in the adenoma to > 60% in the anaplastic carcinoma.

Whole-exome sequencing was performed separately on DNA extracted from the three tissue components: normal thyroid tissue, adenoma and anaplastic carcinoma. An identical *HRAS* c.181A > G (p.Q61K) hotspot mutation was present in both the follicular adenoma and the anaplastic carcinoma, with variant allele frequencies (VAFs) of 31.1% and 7.9%, respectively. This mutation was absent in the matched normal thyroid, establishing that the two tumor components are clonally related. In addition to *HRAS*, ten other shared mutations were detected in both the

adenoma and the carcinoma (Table 1), involving *CDA*, *ADD2*, *ABHD14B*, *TFDP2*, *ALDH1L2*, *ENDOU*, *PLEKHA4*, *ZNF699*, *MBTPS2*, and *SOX3*. Like *HRAS*, the VAFs of these mutations were lower in the carcinoma than in the adenoma, consistent with the low tumor cell fraction in the anaplastic component. As a known tumor driver gene mutation, *TP53* c.A245T (p.H82L) missense mutation was detected in anaplastic carcinoma with a VAF of 8.2%, but was not detected in the adenoma component.

Table 1
Whole exome sequencing detected gene mutations in thyroid follicular adenoma and anaplastic carcinoma.

Tumor	Chromosome	Position	Reference	Alteration	GeneName	cDNA	Protein	Variant classification	Variant allele fraction
adenoma	1	20944959	G	A	CDA	c.G339A	p.W113X	stopgain	0.360
carcinoma	1	20944959	G	A	CDA	c.G339A	p.W113X	stopgain	0.051
carcinoma	1	214178596	C	G	PROX1	c.C1814G	p.T605S	missense mutation	0.131
adenoma	1	154218829	A	G	UBAP2L	c.A992G	p.N331S	missense mutation	0.288
adenoma	2	70906059	A	G	ADD2	c.T1208C	p.F403S	missense mutation	0.315
carcinoma	2	70906059	A	G	ADD2	c.T1208C	p.F403S	missense mutation	0.076
carcinoma	2	136393737	G	A	R3HDM1	c.G719A	p.R240Q	missense mutation	0.065
adenoma	2	61541844	T	A	USP34	c.A3418T	p.S1140C	missense mutation	0.109
adenoma	3	52007997	A	C	ABHD14B	c.T81G	p.S27R	missense mutation	0.403
carcinoma	3	52007997	A	C	ABHD14B	c.T81G	p.S27R	missense mutation	0.106
adenoma	3	141678557	G	A	TFDP2	c.C602T	p.A201V	missense mutation	0.382
carcinoma	3	141678557	G	A	TFDP2	c.C602T	p.A201V	missense mutation	0.061
carcinoma	5	151178834	C	A	G3BP1	c.C803A	p.T268N	missense mutation	0.053
adenoma	6	123101532	C	T	FABP7	c.C170T	p.T57I	missense mutation	0.329
carcinoma	7	6230078	A	C	CYTH3			splicing mutation	0.231
carcinoma	7	26233255	C	T	HNRNPA2B1	c.G781A	p.G261R	missense mutation	0.080
carcinoma	7	128000003	C	T	PRRT4	c.G43A	p.V15I	missense mutation	0.080
adenoma	11	533875	G	T	*HRAS*	c.C181A	p.Q61K	missense mutation	0.311
carcinoma	11	533875	G	T	*HRAS*	c.C181A	p.Q61K	missense mutation	0.079
adenoma	11	64564756	T	C	MAP4K2	c.A1267G	p.S423G	missense mutation	0.071
adenoma	12	105425571	C	A	ALDH1L2	c.G2386T	p.G796W	missense mutation	0.385
carcinoma	12	105425571	C	A	ALDH1L2	c.G2386T	p.G796W	missense mutation	0.068
adenoma	12	48105471	G	A	ENDOU	c.C871T	p.P291S	missense mutation	0.359
carcinoma	12	48105471	G	A	ENDOU	c.C871T	p.P291S	missense mutation	0.073
adenoma	15	37375993	C	T	MEIS2	c.G694A	p.G232R	missense mutation	0.165
adenoma	17	38562659	C	A	TOP2A	c.G1930T	p.E644X	stopgain	0.128

Tumor	Chromosome	Position	Reference	Alteration	GeneName	cDNA	Protein	Variant classification	Variant allele fraction
carcinoma	17	7578208	T	A	TP53	c.A245T	p.H82L	missense mutation	0.082
carcinoma	17	1630664	G	A	WDR81	c.G2411A	p.R804Q	missense mutation	0.089
adenoma	19	49362924	G	A	PLEKHA4	c.C494T	p.P165L	missense mutation	0.380
carcinoma	19	49362924	G	A	PLEKHA4	c.C494T	p.P165L	missense mutation	0.292
adenoma	19	9406656	T	C	ZNF699	c.A1424G	p.Y475C	missense mutation	0.298
carcinoma	19	9406656	T	C	ZNF699	c.A1424G	p.Y475C	missense mutation	0.052
adenoma	21	45681141	A	T	DNMT3L	c.T2A	p.M1?	startloss	0.329
adenoma	22	50657289	G	C	TUBGCP6	c.C4664G	p.P1555R	missense mutation	0.267
adenoma	X	20148726	C	G	EIF1AX			splicing mutation	0.143
adenoma	X	21886665	T	A	MBTPS2	c.T751A	p.Y251N	missense mutation	0.368
carcinoma	X	21886665	T	A	MBTPS2	c.T751A	p.Y251N	missense mutation	0.110
adenoma	X	139586763	G	A	SOX3	c.C463T	p.R155C	missense mutation	0.436
carcinoma	X	139586763	G	A	SOX3	c.C463T	p.R155C	missense mutation	0.114

The targeted PCR test using a thyroid-specific 12-gene panel was employed to compare the differences in genetic alterations between adenomas and anaplastic carcinomas. *TERT* promoter mutations (C250T) were identified in ATC, but not in the adenoma component. No *BRAF* V600E or other common thyroid cancer driver mutations was found in both components.

Discussion

An 83-year-old female underwent thyroidectomy for a long-standing thyroid nodule that had recently enlarged. The resected specimen contained three distinct components: normal thyroid, a follicular adenoma, and an anaplastic carcinoma with squamous differentiation. Because all three were present in the same specimen, we were able to directly compare their genetic profiles, providing an unusual opportunity to trace the mutations that drove a benign tumor to become an aggressive carcinoma.

Whole-exome sequencing identified an identical *HRAS* c.181A>G (p.Q61K) hotspot mutation in both the adenoma and the carcinoma, confirming their clonal relatedness. The *HRAS* mutation was the only canonical thyroid cancer driver present in the adenoma, suggesting that *RAS* activation was sufficient to initiate follicular proliferation but insufficient to produce a malignant phenotype. Two additional driver mutations—*TP53* c.245A>T (p.H82L) and a *TERT* promoter C250T mutation—were detected exclusively in the anaplastic carcinoma. This mutational profile fits the stepwise genetic model of anaplastic transformation in follicular-patterned thyroid lesions, in which an early RAS mutation is followed by TP53 and TERT promoter mutations.

The variant allele frequencies of *HRAS* (7.9%) and *TP53* (8.2%) in the carcinoma were nearly identical, indicating that the *TP53* mutation arose within the ancestral *HRAS*-mutant clone. Both VAFs were substantially lower than the *HRAS* VAF in the adenoma (31.1%). This difference is best explained by the low tumor cell content of the anaplastic component. Grossly, the carcinoma was largely necrotic with only limited viable tumor, and microscopically the tumor cells were sparse and separated by abundant stroma and inflammatory infiltrate. Assuming both mutations are heterozygous—as is typical for *HRAS* and *TP53* in thyroid carcinoma—a VAF of approximately 8% suggests that only 15–20% of the extracted DNA was tumor-derived, an estimate consistent with the histologic appearance. The *TERT* promoter C250T mutation, detected by targeted PCR, was also restricted to the carcinoma. The co-occurrence of *TP53* and TERT promoter mutations is well documented in ATC [6, 7], and their exclusive presence in the malignant component marks these events as the likely drivers of anaplastic transformation.

The spatial relationship between the adenoma and carcinoma further supports a direct clonal

evolution rather than a collision tumor. The adenoma was a well-circumscribed, encapsulated nodule with a thick fibrous capsule (0.2–0.3 cm), and the carcinoma appeared as a discrete, ill-defined area within it, largely necrotic. This arrangement, together with the shared *HRAS* mutation, indicates that the carcinoma arose directly from the adenoma. The presence of additional shared mutations—*CDA, ADD2, ABHD14B, TFDP2, ALDH1L2, ENDOU, PLEKHA4, ZNF699, MBTPS2, and SOX3*—further reinforces the clonal relationship, although none of these are established thyroid cancer drivers.

Most ATCs are thought to arise from pre-existing papillary thyroid carcinomas, and the progression from *BRAF*-mutant papillary carcinoma to *TP53/TERT*-mutant ATC is well characterized. Our case suggests an alternative route: a *RAS*-driven follicular adenoma can evolve directly into ATC upon acquiring *TP53* and *TERT* promoter mutations, bypassing a recognizable differentiated carcinoma intermediate. This pathway, while uncommon, may be underrecognized, particularly in elderly patients whose long-standing nodules undergo rapid enlargement. From a clinical standpoint, this case illustrates a practical point: the sudden growth of a stable, presumably benign nodule in an older patient should prompt urgent investigation, as it may signal the acquisition of high-risk mutations and impending anaplastic transformation.

The immunohistochemical findings mirrored the genomic data and reinforced the morphologic impression of stepwise dedifferentiation. Thyroglobulin, TTF-1, and PAX8 were diffusely positive in the adenoma but largely lost in the anaplastic carcinoma, confirming loss of follicular differentiation at the protein level. The Ki-67 labeling index increased from approximately 5% in the adenoma to over 60% in the carcinoma, consistent with the accumulation of *TP53* and *TERT* promoter mutations and explaining the rapid clinical growth. The squamous areas were diffusely positive for p40 and CK5/6,

confirming squamous differentiation. These squamous foci were intimately admixed with undifferentiated spindle and giant cell areas and shared the same *HRAS*, TP53, and TERT mutations, indicating that the squamous phenotype arose from the same clone. The emergence of squamous differentiation in the setting of *TP53* mutation raises the possibility of lineage infidelity. In this phenomenon, loss of p53 function permits aberrant activation of alternative transcriptional programs, a concept previously implicated in other organs [8–10]. Our findings are consistent with this model.

In summary, this case provides direct genomic evidence that a *RAS*-driven follicular adenoma can evolve into an anaplastic carcinoma through the sequential acquisition of *TP53* and *TERT* promoter mutations. The coexistence of adenoma and carcinoma within the same encapsulated nodule, together with matched molecular data, reconstructs the clonal evolution of anaplastic transformation and underscores the clinical importance of rapid growth in long-standing thyroid nodules.

Declarations

Funding: No funding was received for this study.

Competing interests: The authors declare no competing interests.

Ethics approval: This study was performed in line with the principles of the Declaration of Helsinki. This study was approved by the institutional ethics committee of The 960th Hospital of the PLA Joint Logistic Support Force.

Consent to participate: Written informed consent was obtained from the patient for participation in this study.

Consent to publish: Written informed consent was obtained from the patient for publication of this case report and any accompanying images.

Data availability: The raw sequence data reported in this paper have been deposited in the Genome Sequence Archive (Genomics, Proteomics & Bioinformatics 2025) in National Genomics Data Center (Nucleic Acids Res 2025), China National Center for Bioinformation / Beijing Institute of Genomics, Chinese Academy of Sciences (GSA-Human:HRA021209) that are publicly accessible at https://ngdc.cncb.ac.cn/gsa-human[11–12].

Authors' contributions: Huixuan Wang performed the histological and immunohistochemical analyses and drafted the manuscript. Yongcheng Cao conducted the molecular experiments and data analysis. Peifeng Li conceived and supervised the study, interpreted the data, and critically revised the manuscript. All authors read and approved the final manuscript.

References

1. Chintakuntlawar AV, et al. Diagnosis and Management of Anaplastic Thyroid Cancer. Endocrinol Metab Clin North Am. 2019;48(1):269–84. https://doi.org/10.1016/j.ecl.2018.10.010.
2. Mao Y, Xing M. Recent incidences and differential trends of thyroid cancer in the USA. Endocr Relat Cancer. 2016;23(4):313–22. https://doi.org/10.1530/ERC-15-0445.

3. Wiseman SM, et al. Anaplastic transformation of thyroid cancer: review of clinical, pathologic, and molecular evidence provides new insights into disease biology and future therapy. Head Neck. 2003;25(8):662–70. https://doi.org/10.1002/hed.10277. Digital Object Identifier (DOI).
4. Xu B, Ghossein R. Genomic Landscape of poorly Differentiated and Anaplastic Thyroid Carcinoma. Endocr Pathol. 2016;27(3):205–12. https://doi.org/10.1007/s12022-016-9445-4.
5. Landa I, et al. Genomic and transcriptomic hallmarks of poorly differentiated and anaplastic thyroid cancers. J Clin Invest. 2016;126(3):1052–66. https://doi.org/10.1172/JCI85271.
6. He Y, et al. Dedifferentiation and Redifferentiation of Follicular-Cell-Derived Thyroid Carcinoma: Mechanisms and Therapeutic Implications. Biomedicines. 2025;13(12). https://doi.org/10.3390/biomedicines13122982.
7. Leandro-García LJ, Landa I. Mechanistic Insights Thyroid Cancer Progression Endocrinol. 2023;164(9). https://doi.org/10.1210/endocr/bqad118.
8. Scheistrøen M et al. *p53 protein expression in squamous cell carcinoma of the vulva.* Cancer, 1999. 85(5): pp. 1133–8. https://doi.org/10.1002/(SICI)1097-0142(19990301)85:5%3C1133::AID-CNCR17>3.0.CO;2-T
9. Zhang L, et al. Aberrant Cytoplasmic p53 Staining in Oral Squamous Cell Carcinoma and Dysplasia: A Clinicopathologic and Molecular Study. Am J Surg Pathol. 2025;49(12):1216–24. https://doi.org/10.1097/PAS.0000000000002471.
10. Zhong L, et al. TP53 Mutations in Esophageal Squamous Cell Carcinoma. Front Biosci (Landmark Ed). 2023;28(9):219. https://doi.org/10.31083/j.fbl2809219.
11. Genomics. Family in 2025: A Broadened Sharing Platform for Multi-Omics and Multimodal Data. Proteom Bioinf. 2025;23(4):qzaf072. https://doi.org/10.1093/gpbjnl/qzaf072.
12. Database Resources of the National Genomics Data Center, China National Center for Bioinformation in 2026. Nucleic Acids Res. 2026;54(D1):D28–47. https://doi.org/10.1093/nar/gkaf1172.

Figures

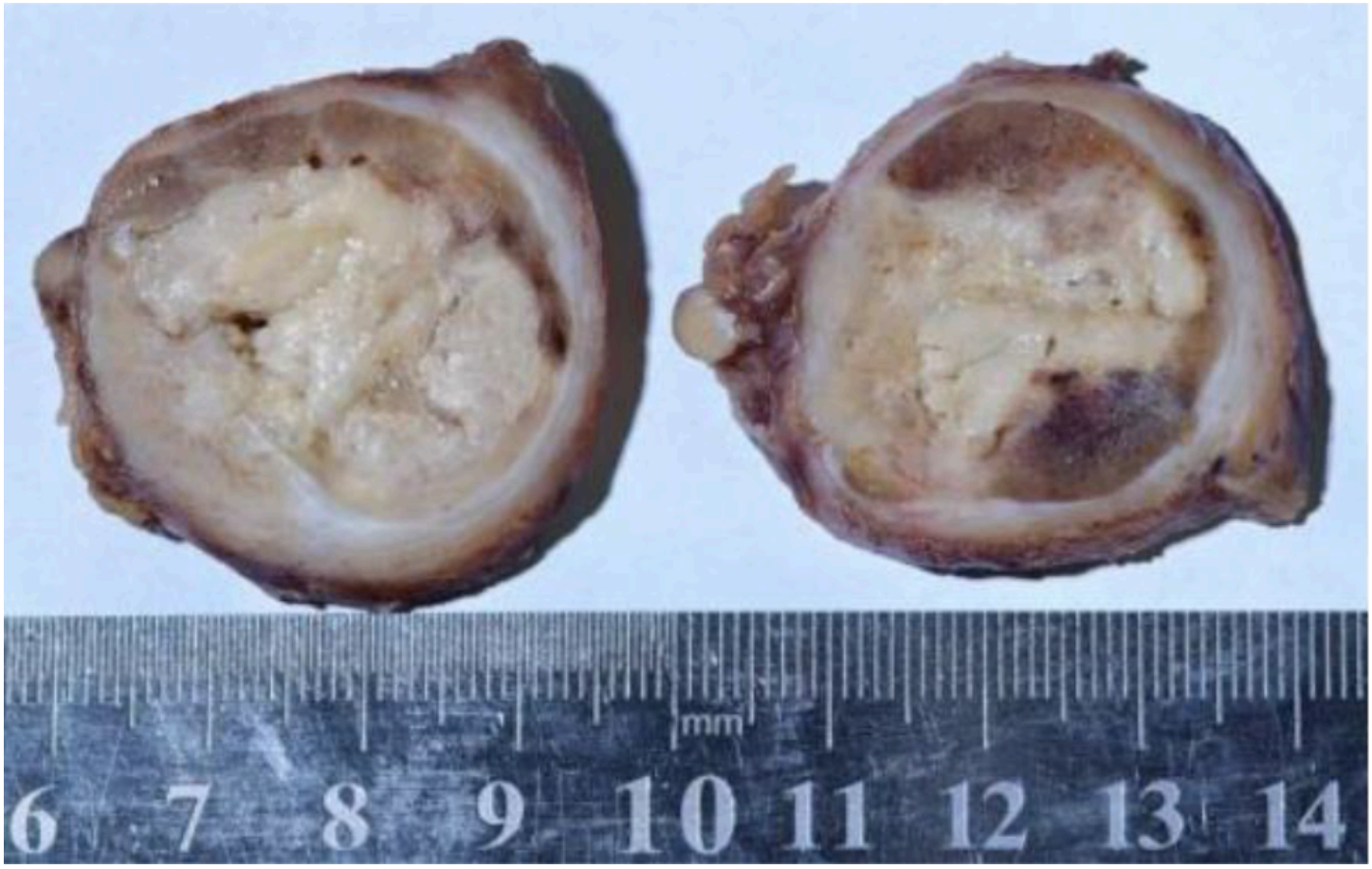


Figure 1

Gross specimen. The cut surface shows a well-encapsulated follicular adenoma with a thick fibrous capsule and a predominantly tan cut surface. A discrete area within the adenoma is largely necrotic, with small residual foci of gray-white, firm viable tumor representing the anaplastic carcinoma.

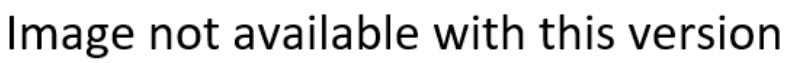


Figure 2

Histology and immunohistochemistry of the follicular thyroid adenoma and anaplastic carcinoma. (A, B) H&E staining of the follicular adenoma (A) and anaplastic carcinoma with squamous differentiation (B). (C, D) Thyroglobulin. (E, F) p53. (G, H) p40. (I, J) Ki-67. The adenoma shows intact thyroglobulin expression, negative p40, wild-type p53 pattern, and low Ki-67 index. In contrast, the carcinoma shows complete loss of thyroglobulin, diffuse p40 positivity in squamous areas, mutant-pattern p53 staining, and markedly elevated Ki-67 index.